

# Synthesis and characterization of hyperbranched polymers via $\text{Cp}_2\text{TiCl}$ -catalyzed self-condensing vinyl polymerization using glycidyl methacrylate as inimer

Xiao-hui Liu<sup>a</sup>, Zhong-min Dong<sup>a,b</sup>, Xiu-lan Tang<sup>c</sup>, Yue-sheng Li<sup>a,c,\*</sup>

<sup>a</sup>State Key Laboratory of Polymer Physics and Chemistry, Changchun Institute of Applied Chemistry, Chinese Academy of Sciences, Changchun 130022, China

<sup>b</sup>Graduate School of the Chinese Academy of Sciences, Changchun Branch, Changchun 130022, China

<sup>c</sup>College of Environment & Chemical Engineering, Yanshan University, Qinhuangdao 066004, China

## ARTICLE INFO

### Article history:

Received 16 August 2009

Received in revised form

22 December 2009

Accepted 29 December 2009

Available online 11 January 2010

### Keywords:

Hyperbranched

Self-condensing vinyl polymerization

Epoxide radical ring opening

## ABSTRACT

Hyperbranched polymers were produced using glycidyl methacrylate (GMA)/ $\text{Cp}_2\text{TiCl}_2/\text{Zn}$  as self-condensing vinyl polymerization (SCVP) system. The polymerization is firstly initiated by the epoxide radical ring opening catalyzed by  $\text{Cp}_2\text{Ti(III)Cl}$  generated in situ via the reaction of  $\text{Cp}_2\text{TiCl}_2$  with Zn. By optimizing the molar ratio of the SCVP inimer (GMA) to the mediator ( $\text{Cp}_2\text{Ti(III)Cl}$ ), the active propagation chains are reversibly transformed to the dormant species and the cross-linking does not occur until a higher level of monomer conversion (ca. 80%). We detail this facile one-step polymerization technique to prepare highly branched polymers with a multiplicity of particular end reactive functionalities including Ti alkoxide, hydroxyl and vinyl functional groups, which differs from most previously reported SCVP systems.

© 2010 Elsevier Ltd. All rights reserved.

## 1. Introduction

Hyperbranched polymers have evolved into an important research field in the past decade because they possess many unique properties including low viscosity, high functionality and excellent solubility compared with their linear analogs [1]. Initially, most hyperbranched polymers were prepared via the self-polycondensation reaction of multifunctional  $\text{AB}_x$  type monomers containing carboxyl, hydroxyl and amine groups etc [2]. However, this method cannot control the molecular weight and hyperbranched structure of the resultant polymers due to lacking living/controlled polymerization characteristics. Moreover, there were few routes to produce hyperbranched polymers originated from vinyl monomers [3]. Until 1995, an important discovery coining as self-condensing vinyl polymerization (SCVP) in this area was reported by Fréchet and his coworkers [4].

The SCVP methodology first need employ an *initiator monomer* (*inimer*), which possesses general  $\text{AB}^*$  structure comprising a double bond (A) and a latent initiating site ( $\text{B}^*$ ) for vinyl polymerization. Propagation takes place at either A or after the initiation of  $\text{B}^*$ , resulting in branching points and eventually producing hyperbranched polymers. The hyperbranched polymers can also be

prepared by copolymerizing conventional vinyl monomers with inimer. The degree of branching was controlled by tuning the ratio of monomer to SCVP inimer. Concerning the versatility of this approach, it has subsequently been expanded successfully from cation [4] to anionic [5], group-transfer [6], ATRP [6b,7], RAFT [8], and nitroxide-mediated polymerization [9]. However, there are still some disadvantages for SCVP method, such as, this process usually requires tremendous efforts to design and synthesize the expensive, tailored vinyl monomer (inimer) with special functional groups.

Recently,  $\text{Cp}_2\text{Ti(III)Cl}$ -catalyzed epoxide radical ring opening (RRO) was successfully used to initiate radical polymerization of styrene (St) and graft copolymerization of (meth)acrylate derivatives [10,11]. These polymerizations proceed in a living fashion and produced well-defined polymers. Glycidyl methacrylate (GMA) is an important kind of commercial functional monomer as it contains both a double bond and an epoxide group. Therefore, it is potential for serving as a facile SCVP inimer for preparing hyperbranched polymers. Initially, Asandei and his coworkers reported the homopolymerization of GMA catalyzed by  $\text{Cp}_2\text{Ti(III)Cl}$ . Due to a large excess of epoxide groups by comparison with available  $\text{Cp}_2\text{Ti(III)Cl}$ , the mediator  $\text{Cp}_2\text{Ti(III)Cl}$  consumed fast and completely at the start of the polymerization [12a]. As a result, the cross-linking readily occurred even at a low monomer conversion of ca. 20%. To solve this problem, Pan's group introduced ATRP mediators ( $\text{CuBr}_2/\text{bpy}$ ) to control the homopolymerization of GMA or its copolymerization with St, with the purpose to prevent potential cross-linking [12b]. In nature, the polymerization follows

\* Corresponding author. College of Environment & Chemical Engineering, Yanshan University, Qinhuangdao 066004, China.

E-mail address: [ysli@ciac.jl.cn](mailto:ysli@ciac.jl.cn) (Y.-s. Li).

a reverse ATRP mechanism. Consequently, a significant improvement in monomer conversions was obtained. However, they are still limited to ca. 50%.

In the present paper, hyperbranched polymers with higher monomer conversions (ca. 80%) were generated in one-pot RRO copolymerization of St and GMA where  $\text{Cp}_2\text{Ti(III)Cl}$  is employed as the exclusive mediator and no other LRP mediator is needed. The only key requirement is to optimize the molar ratio of the inimer (GMA) to the mediator ( $\text{Cp}_2\text{Ti(III)Cl}$ ) for preventing cross-linking reaction. Furthermore, the evolution of molecular dimension and branched architecture were confirmed by a conventional size exclusion chromatography (SEC), and a triple SEC (Tri-SEC) as well as  $^1\text{H}$  NMR spectra analyses.

## 2. Experiment

### 2.1. Materials

After passing through a column of alumina to remove the inhibitor, GMA, St, 4-methylstyrene (MSt), and *p*-chloromethyl styrene (CMS) were distilled prior to use. *N*-phenylmaleimide (NPMI) was recrystallized from acetone twice, and maleic anhydride (MA) was purified by sublimation. Bis(cyclopentadienyl)titanium dichloride ( $\text{Cp}_2\text{TiCl}_2$ , Acros), Zn powder (Beijing Chemical Factory), and styrene oxide (SO, Acros) were used as received. 1,4-Dioxane was distilled over Na/benzophenone.

### 2.2. Polymerization

A Schlenk tube was filled with  $\text{Cp}_2\text{TiCl}_2$ , Zn,  $\text{CaH}_2$  (<10 mg, moisture scavenger), and dioxane was degassed using three freeze-pump-thaw cycles prior to filling with dry argon. The reduction of  $\text{Cp}_2\text{TiCl}_2$  was finished in 10 min at room temperature and was accompanied by the characteristic lime-green color of  $\text{Cp}_2\text{Ti(III)Cl}$ . The tube was then cooled to  $-78^\circ\text{C}$  in an acetone/dry ice bath. Degassed St and GMA were injected through the sidearm, and the mixture was redegassed by three freeze-pump-thaw cycles. The polymerization was performed at  $90^\circ\text{C}$  in a thermostated oil bath. After a desired reaction time, the polymerization was quenched by liquid nitrogen. The content of the Schlenk tube was diluted with THF and precipitated into a large excess of methanol. The resulting polymer was filtered and dried *in vacuo* at  $30^\circ\text{C}$ . The polymer yields were determined gravimetrically.

### 2.3. Hydrolysis of hyperbranched polystyrene

0.5 g of the resultant hyperbranched polystyrene ( $M_w = 619$  kDa,  $\text{PDI} = 9.08$  determined by Tri-SEC) was dissolved in 10 mL of dioxane. 0.8 mL of 37% HCl was added to the mixture, and the mixture was refluxed at  $90^\circ\text{C}$  for 48 h. Solvent was then removed by rotary evaporator and the crude product was extracted by  $\text{CH}_2\text{Cl}_2$ . After being removed the solvent, a white polymer was afforded and vacuum dried. Yield: 91%;  $M_w = 8.3$  kDa,  $\text{PDI} = 1.20$  determined by Tri-SEC.

### 2.4. Characterization

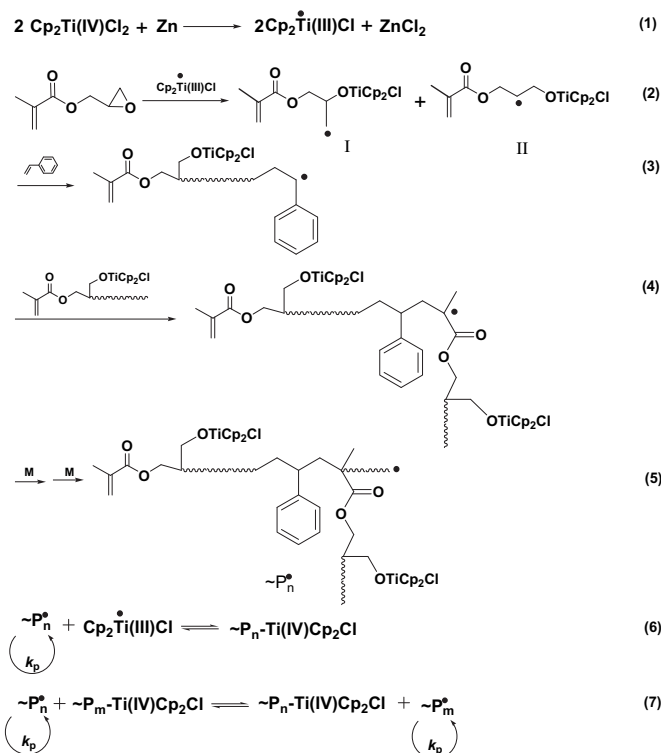
$^1\text{H}$  NMR spectra were recorded on a Bruker 300-MHz spectrometer with  $\text{CDCl}_3$  as the solvent and tetramethylsilane (TMS) as the internal standard. The weight-average molecular weights ( $M_w$ ) and polydispersity indices (PDIs) of all samples were measured on a size exclusion chromatography (SEC) system, which consists of a Waters 510 HPLC pump, three Waters Ultrastaygel columns ( $500$ ,  $10^3$ , and  $10^5$ ), and a Waters 2414 RI detector, with THF as the eluent at a flow rate of 1.0 mL/min. The molecular weight analysis was

performed at  $40^\circ\text{C}$  and calibrated by narrow polystyrene (PSt) standards. Additional measurements of  $M_w$ , PDI, and Mark-Houwink exponent  $\alpha$  values were performed on a Triple Detection Size Exclusion Chromatography (Tri-SEC) supplied by a Waters 1525 separation module (Waters Corp.) connected with M302 triple detector array (Viscotek Corp., Houston, TX), a combination of refractive index, light scattering (LS angle,  $7^\circ$  (LALS) and  $90^\circ$  (RALS), laser wavelength,  $\lambda = 670$  nm) and viscosity detector. Two mixed bed SEC columns ( $\text{GMH}_{\text{HR-M}}$ ,  $\text{GMH}_{\text{HR-H}}$ , Viscotek Corp.) were used. THF was used as the mobile phase at a flow rate of 1.0 mL/min and the column oven temperature was set to  $30^\circ\text{C}$ .

## 3. Results and discussion

### 3.1. Synthesis of hyperbranched polystyrene initiated via $\text{Cp}_2\text{Ti(III)Cl}$ -catalyzed radical ring opening (RRO) of GMA

Scheme 1 outlines the proposed polymerization mechanism for the synthesis of hyperbranched polystyrene.  $\text{Cp}_2\text{Ti(III)Cl}$  was prepared *in situ* via the reduction of  $\text{Cp}_2\text{TiCl}_2$  with Zn at room temperature, as evidenced by a characteristic color change from red to lime-green [12]. The soluble paramagnetic  $\text{Cp}_2\text{Ti(III)Cl}$  complex is an excellent one electron-transfer agent that can catalyze a variety of radical reactions including the RRO of epoxides [13]. Addition of GMA/St mixture into  $\text{Cp}_2\text{Ti(III)Cl}$  solution leads to the rapid formation of a red-orange color associated with Ti alkoxides radical ( $\text{Cp}_2\text{TiClOR}^\bullet$ ) and indicating the occurrence of the epoxide radical ring opening (RRO) reaction. The  $\text{Cp}_2\text{Ti(III)Cl}$ -catalyzed RRO of GMA generates a mixture of reactive, primary (I) and secondary C-centered radicals (II) derived from the regioselectivity of the RRO reaction that have the same thermodynamic stabilization as the corresponding alkyl radicals [14]. Generally, the secondary radical is favored [15]. For simplicity, the most important active species (II) are showed in Scheme 1. The addition of such radicals to the double



**Scheme 1.** Strategy for polymerization of St initiated from  $\text{Cp}_2\text{Ti(III)Cl}$ -catalyzed radical ring opening of GMA.

bonds of St is expected to be fast. Addition of the propagating radical polymer chain onto the  $\text{H}_2\text{C}=\text{C}$  of the inimer and/or the macromonomer methacrylate allows for the formation of hyperbranched polymers (steps 4 and 5). The controlled/living nature of such polymerizations is based on a dissociation–combination (DC, step 6) and degenerative transfer (DT, step 7) mechanisms [10]. The key feature of the SCVP polymerization is that the concentration of the active propagating radical chains remains low. As a result, cross-linking can be prevented.

All polymerizations were conducted in a one-pot procedure at  $90^\circ\text{C}$  as this reaction temperature has been demonstrated to be optimal for the radical polymerization of St initiated by  $\text{Cp}_2\text{Ti(III)Cl}$  and SCVP has also been shown to suppress the Trommsdorff effect [10,11]. The results are presented in Table 1. A control polymerization experiment is presented in entry 1. In the absence of the inimer GMA, the polymerization of St initiated by  $\text{SO}/\text{Cp}_2\text{TiCl}_2/\text{Zn}$  produced a linear PSt with a molecular weight (MW) close to the theoretical value and a polydispersity index (PDI) as low as 1.35 measured by conventional SEC technique. In contrast, the RRO polymerizations of St/GMA produce the polymers with higher MWs than the theoretical values and higher PDIs (2.10–3.32, entries 2–7). Furthermore, it is also noted that the  $[\text{GMA}]/[\text{Cp}_2\text{TiCl}_2]$  molar ratios significantly influenced the RRO polymerization outcomes. At a higher molar ratio of GMA to  $\text{Cp}_2\text{TiCl}_2$  (1:2, entry 2), low yield of hyperbranched polystyrene were obtained. Gelation was obtained when the yield of polymer exceeded 40%. According to the reaction mechanism described in Scheme 1, two equivalents of  $\text{Cp}_2\text{Ti(III)Cl}$  are necessary for the controlled/living polymerization process to be efficient [10]. Entries 2 to 5 show that when the concentration of  $\text{Cp}_2\text{Ti(III)Cl}$  exceeds 2 equivalents, the yield of soluble hyperbranched polystyrene is significantly increased from 38.5% to 78.6%. Interestingly, the use of a large excess of  $\text{Cp}_2\text{Ti(III)Cl}$  causes the polymer yield to be significantly reduced (entries 6 and 7). This study has shown that the optimal molar ratio of  $[\text{St}]/[\text{GMA}]/[\text{Cp}_2\text{Ti(III)Cl}]$  is 100:1:4.

$^1\text{H}$  NMR spectra reveal the convincing information for elucidating the polymerization proceeding (entry 5 in Table 1), as shown in Fig. 1. The presence of GMA end group on the PSt backbone is clearly supported by the methacrylate double bond resonance ( $\text{CH}_2=\text{C}(\text{CH}_3)\text{COO}-$ ,  $\delta = 5.25$  and 5.80 ppm). Moreover, the methylene protons (peak **d'**) adjacent to hydroxyl groups derived from hydrolysis reaction of Ti alkoxide are observed at ca. 3.80 ppm. The signals at ca. 2.0 ppm are assigned to methylene and methine protons (**d**, **e'**), corresponding to the two paths of epoxide ring opening. Importantly, the peaks of the methacrylate double bond derived from GMA in the macromolecular chain trended to disappear with the polymerization proceeding (as shown in the inset spectra in Fig. 1), and the relative intensity of peak **a** with respect to the sum of peaks **c**, **c'**, **d'** and **e** also decreases as the polymerization

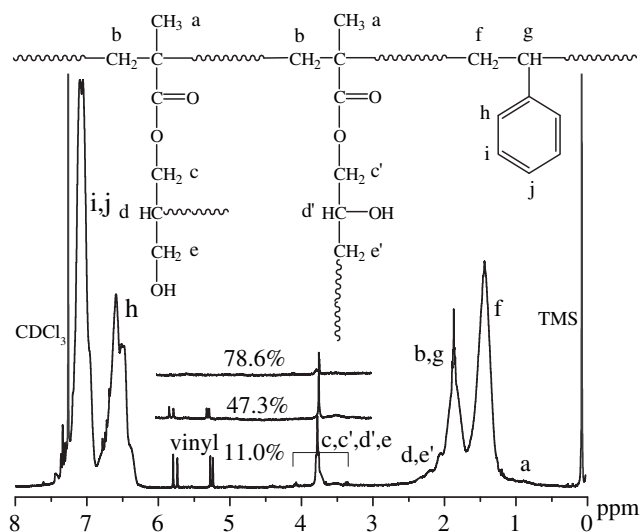


Fig. 1.  $^1\text{H}$  NMR spectra of hyperbranched PSt via the initiation of  $\text{Cp}_2\text{Ti(III)Cl}$ -catalyzed RRO of GMA at different monomer conversions.  $[\text{St}]/[\text{GMA}]/[\text{Cp}_2\text{TiCl}_2]/[\text{Zn}] = 100:1:4:8$ ,  $T = 90^\circ\text{C}$ ,  $\text{St}/\text{solvent} = 1/1$  (v/v), solvent: dioxane.

proceeds, which provide the solid evidence that the methacrylate double bond was indeed involved in the formation of hyperbranched structure. These observations demonstrate that hyperbranched PSt was synthesized via the initiation of  $\text{Cp}_2\text{Ti(III)Cl}$ -catalyzed RRO of GMA, and the hyperbranched polymers possess a multiplicity of end reactive functionalities including Ti alkoxide, hydroxyl and vinyl functional groups. As proposed by Rimmer and his coworkers, the degree of branching (DB) can be obtained by comparison of the St aromatic protons to the protons of **a**, **b**, **c**, **d**, **e**, **c'**, **d'**, **e'**, corresponding to the GMA unit. However, the concentration of these protons is low and they are overlapped with other protons from St. Therefore, the DB values are difficultly determined [8b].

The kinetic of the polymerization in entry 4 Table 1 was followed. Fig. 2 shows that the yields of polystyrene steadily increase with time to reach 78.6% after 8 h. The pseudo first-order kinetic plot is linear and indicates that the concentration of the growing radical chains ( $\text{Pn}^*$ ) is constant [16].  $M_n$  and PDI values are also plotted versus monomer conversions in Fig. 3. The molecular weights of the resultant hyperbranched polymers increase with monomer conversions, which indicates that St polymerization

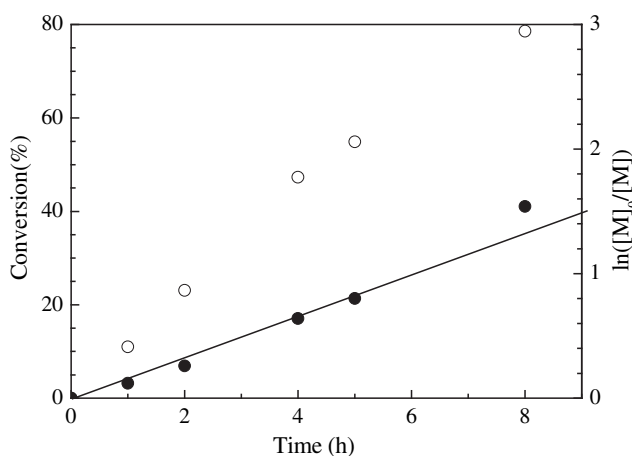


Fig. 2. Plots of monomer conversion ( $\circ$ ) and  $\ln([M]_0/[M])$  ( $\bullet$ ) versus reaction time.  $[\text{St}]/[\text{GMA}]/[\text{Cp}_2\text{TiCl}_2]/[\text{Zn}] = 100:1:4:8$ ,  $T = 90^\circ\text{C}$ ,  $\text{St}/\text{solvent} = 1/1$  (v/v), solvent: dioxane.

Table 1  
Polymerization results of styrene initiated from  $\text{Cp}_2\text{Ti(III)Cl}$ -catalyzed RRO of GMA<sup>a</sup>.

Entry	$[\text{St}]/[\text{GMA}]/[\text{Cp}_2\text{TiCl}_2]/[\text{Zn}]$	Time (h)	Conv. (%)	SEC results			Tri-SEC results			$\alpha^b$
				$M_n$ (kDa)	$M_w$ (kDa)	PDI	$M_n$ (kDa)	$M_w$ (kDa)	PDI	
1	Control <sup>c</sup>	24	74.7	12.0	16.2	1.35	13.0	17.2	1.32	0.73
2	100:1:2:4	3	38.5	24.6	60.5	2.46	125	333	2.67	0.45
3	100:1:2:4	4	45.0	gel						
4	100:1:3:6	5	49.4	15.6	33.4	2.14	80.0	245	3.06	0.49
5	100:1:4:8	8	78.6	30.3	101	3.32	68.2	619	9.08	0.51
6	100:5:10	20	70.0	16.2	36.6	2.26	20.8	47.6	2.29	0.57
7	100:1:6:12	20	60.0	15.0	31.5	2.10	16.7	44.1	2.67	0.63
8	50:1:4:8	6	39.0	10.4	22.0	2.11	9.40	41.6	4.43	0.17
9	200:1:4:8	20	60.0	32.0	92.8	2.90	43.9	280	6.38	0.52

<sup>a</sup> Polymerization conditions:  $T = 90^\circ\text{C}$ ,  $\text{St}/\text{solvent} = 1/1$  (v/v), solvent: dioxane.

<sup>b</sup> Mark–Houwink exponent.

<sup>c</sup>  $[\text{St}]/[\text{SO}]/[\text{Cp}_2\text{TiCl}_2]/[\text{Zn}] = 100:1:2:4$ .

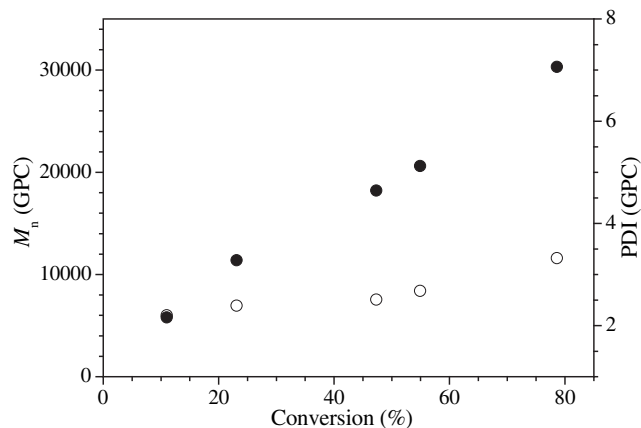


**Fig. 3.** Plots of  $M_n$  (●) and PDI (○) of hyperbranched PSt measured by SEC versus monomer conversion.  $[St]/[GMA]/[Cp_2TiCl_2]/[Zn] = 100:1:4:8$ ,  $T = 90^\circ C$ ,  $St/solvent = 1/1$  (v/v), solvent: dioxane.

initiated from the RRO of GMA exhibits the characteristics of a controlled/living radical polymerization (CRP) [17]. In the case of the molecular weight distributions, they showed a tendency of broadening as a result of the gradual increase of the degree of branching (DB) [18]. The rule can also be observed from the evolution of SEC curves of obtained polymers with the increase of monomer conversions (Fig. 4). At the initial stage of the polymerization, the SEC curves are monomodal and nearly symmetrical. With the increase of the monomer conversions, the traces shift clearly to higher molecular weights. The polymer obtained at 8 h has a PDI of 3.32, and the corresponding SEC trace becomes bimodal. These results may be an indication of the formation of the hyperbranched structure at the latter polymerization stage. The similar phenomena were also observed in synthesis of other hyperbranched polymers [18].

To further demonstrate the hyperbranched structure and the related properties of PSt obtained from  $Cp_2Ti(III)Cl$ -catalyzed RRO of GMA, more accurate Tri-SEC analyses (Fig. 5) equipped with three detectors including refractive index (RI), viscosity (Vis) and light scattering (LS) were performed for PSt with  $M_w = 101$  kDa, and PDI = 3.32 measured by traditional SEC technique. Obviously,

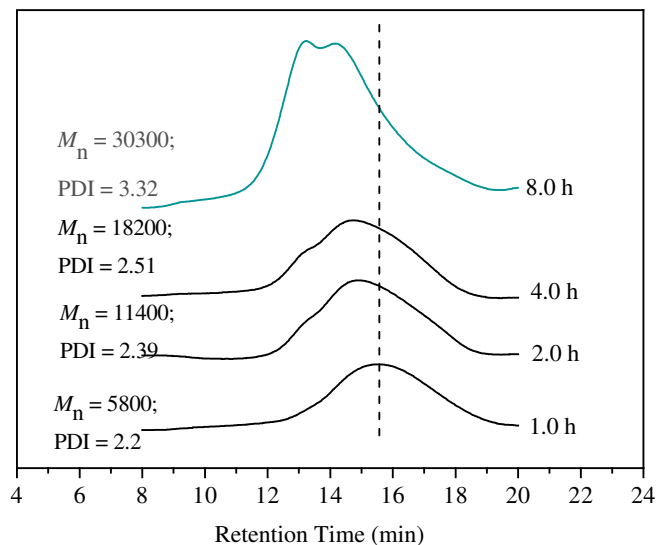


**Fig. 4.** SEC traces of hyperbranched PSt via  $Cp_2Ti(III)Cl$ -catalyzed RRO of GMA at  $90^\circ C$  with polymerization proceeding.  $[St]/[GMA]/[Cp_2TiCl_2]/[Zn] = 100:1:4:8$ ,  $St/solvent = 1/1$  (v/v), solvent: dioxane.

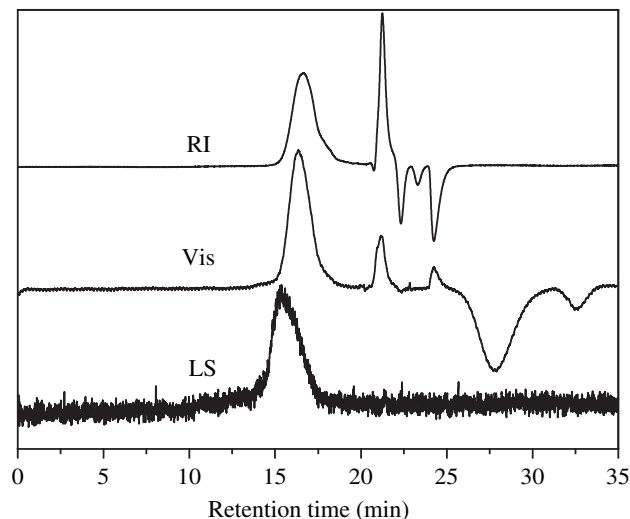


**Fig. 5.** Tri-SEC molar mass distribution curves for hyperbranched PSt via  $Cp_2Ti(III)Cl$ -catalyzed RRO of GMA.

both molecular weight ( $M_w = 619$  kDa) and PDI (9.08) increase dramatically compared with the SEC results, which is in consistent with the reported results [19]. The resultant St polymers also show the unique properties of hyperbranched polymers, i.e., longer retention times due to lower hydrodynamic volumes at the same  $M_w$  values, than the linear counterparts, as shown in Fig. 6 [7f,20].

Furthermore, the corresponding molecular weight versus retention volume curve also provides the proof of hyperbranched architecture (Fig. 7). The plots clearly lies above the linear PSt standard, indicating that at any given retention volume, the molecular weight of the hyperbranched polymer sample is higher than that of the linear analogue [21].

Finally, the hyperbranched characteristics can be conclusively confirmed by the specific solution properties. The intrinsic viscosity (IV) of PSts obtained from GMA mediated polymerization exhibit a lower intrinsic viscosity than that of the linear counterpart in the classical Mark–Houwink plots (Fig. 8). Indeed, the lower Mark–Houwink exponent  $\alpha$  values (0.17–0.63) for PSts obtained by the  $Cp_2Ti(III)Cl$ -catalyzed RRO of GMA compared to the linear PSt standard ( $\alpha = 0.73$ ) implies their compact hyperbranched structure [17b,18a,22].

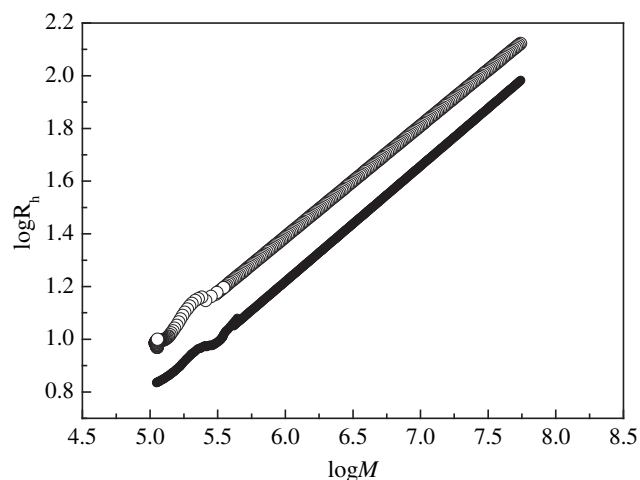


**Fig. 6.** Plot of hydrodynamic radius vs molecular weight for hyperbranched PSt obtained in entry 4 of Table 1 (●) and linear PSt standards (○).

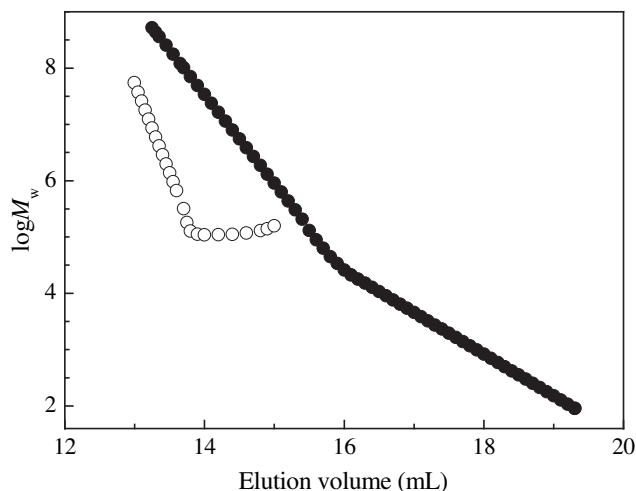


Fig. 7. Plot of the molecular weight vs retention volume for hyperbranched PSt obtained in entry 4 of Table 1 (●) and linear PSt standard (○).

Hydrolysis of the ester linkages in the resultant polymer can also give important information on its structure type. Before hydrolysis, the polymer initiated from GMA has  $M_w$  of 619 kDa, PDI of 9.08, and Mark–Houwink exponent  $\alpha$  value of 0.51 measured by Tri-SEC technique. Conversely, the hydrolyzed product has  $M_w$  of 8.3 kDa, PDI of 1.20 measured by Tri-SEC. Importantly, its Mark–Houwink exponent  $\alpha$  value is 0.73, which is in consistent with the typical values of linear PSt samples. Therefore, the results indicate that the radical polymerization via  $\text{Cp}_2\text{Ti(III)Cl}$ -catalyzed RRO of GMA was unexpectedly well controlled and the generated polymer owned the hyperbranched structure.

### 3.2. Effect of the $[\text{St}]/[\text{GMA}]/[\text{Cp}_2\text{TiCl}_2]$ molar ratios on hyperbranched architecture

Based on earlier results, the resultant PSts synthesized via the initiation of  $\text{Cp}_2\text{Ti(III)Cl}$ -catalyzed RRO of GMA possess hyperbranched architecture (entries 2–9 in Table 1), as evidenced by higher molecular weight (MW) difference between traditional SEC and Tri-SEC results when compared with the control experiment (entry 1 in Table 1). Furthermore, unlike their linear analogue, hyperbranched products exhibit higher PDI values (2.67–9.08 for

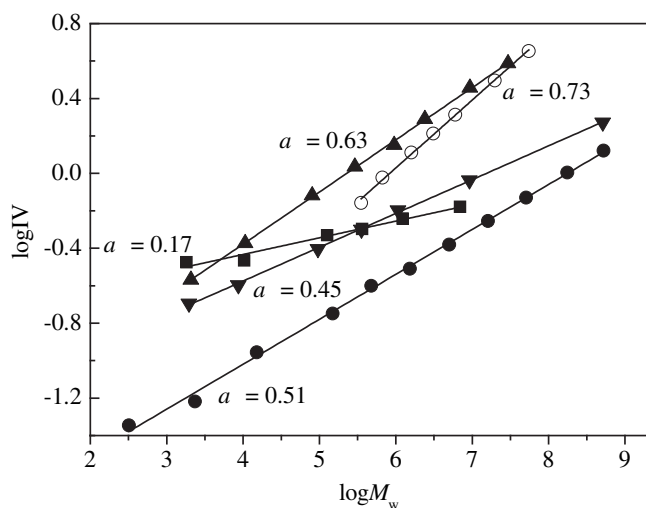


Fig. 8. Plot of intrinsic viscosity vs molecular weight for hyperbranched PSt obtained in entries 2 (▼), 5 (●), 7 (▲), 8 (■) of Table 1 and linear PSt standards (○).

Tri-SEC results), and usually display lower Mark–Houwink exponents (Table 1), characteristic of a hyperbranched structure. However, Mark–Houwink exponents varied greatly. Therefore, it is necessary to investigate the effect of the  $[\text{St}]/[\text{GMA}]/[\text{Cp}_2\text{TiCl}_2]$  molar ratios on hyperbranched architecture.

Fig. 8 shows that the Mark–Houwink slope  $\alpha$  significantly increase from 0.43 to 0.63 with an increase in  $[\text{GMA}]/[\text{Cp}_2\text{TiCl}_2]$  ratio from 1:2 to 1:6 (entries 2, 5 and 7 in Table 1). It indicates that the DB decreases with an increase in the concentration of  $\text{Cp}_2\text{TiCl}_2$ . As discussed above, the decrease of  $[\text{GMA}]/[\text{Cp}_2\text{TiCl}_2]$  implies the improvement of  $\text{Cp}_2\text{Ti(III)Cl}$  species, which can more efficiently convert the active propagation chains into the dormant species. Thus, the active radical concentration was remained in a lower level and the polymerizations would proceed in a more controlled/living fashion. As a result, the branching process was inhibited to a certain extent and the linear propagation route was encouraged. This explanation can also be indirectly confirmed from a linear decrease of MWs accurately determined by Tri-SEC analyses with the decrease of the  $[\text{GMA}]/[\text{Cp}_2\text{TiCl}_2]$  molar ratios.

Moreover, the  $[\text{St}]/[\text{GMA}]$  molar ratios considerably influenced the DBs of hyperbranched polymers. Obviously, the Mark–Houwink exponent  $\alpha$  is 0.17 for a  $[\text{St}]/[\text{GMA}]$  molar ratio of 50:1 (entry 8 in Table 1), which is much lower than that (0.51) for a higher  $[\text{St}]/[\text{GMA}]$  molar ratio (100:1 for entry 5 in Table 1). It must be pointed out that a lower value of 0.17 may also be due to the molecular weight of the PSt being too low to be analyzed accurately as the LS lower detection limit is usually 10 kDa. As a result, any molecular weight distribution below this limit will not give a significant  $\alpha$  value. Moreover, the slope of  $\text{Log IV}$  versus  $\text{Log M}$  obviously decreases (Fig. 8). These results indicate that the decrease of  $[\text{St}]/[\text{GMA}]$  leads to an increase in the concentration of methacrylate vinyl groups  $[\text{CH}_2=\text{C}(\text{CH}_3)\text{C}(=\text{O})\text{O}-]$ , and thus augments the probability of branching or cross-linking. Consequently, the hyperbranched structure produced at a low monomer conversions (39.0%) for a  $[\text{St}]/[\text{GMA}]$  molar ratio of 50:1.

### 3.3. Extension of the $\text{GMA}/\text{Cp}_2\text{TiCl}_2/\text{Zn}$ SCVP system to other monomers

The study of the scope of polymerization mediated by  $\text{GMA}/\text{Cp}_2\text{TiCl}_2/\text{Zn}$  was extended to MSt, CMS, St/NPMI, and St/MA. As presented in entries 2–5 of Table 2, under the same reaction conditions, these polymerizations yielded low-to-high monomer conversions. Noticeably, a fast polymerization rate was observed for CMS. It is possible that the introduction of the halogen element (chlorine) in CMS can considerably accelerate the polymerization initiated by the  $\text{Cp}_2\text{Ti(III)Cl}$ -catalyzed RRO reaction of epoxide. In contrast, a poor polymerization behavior is observed for the copolymerization of St and MA (entry 5), which is induced by the

Table 2  
Polymerization results of other monomers initiated form  $\text{Cp}_2\text{Ti(III)Cl}$ -catalyzed RRO of GMA<sup>a</sup>.

No.	Monomer	Time (h)	Conv. (%)	Tri-SEC results			
				$M_n$ (kDa)	$M_w$ (kDa)	PDI	$\alpha^b$
1	St <sup>c</sup>	8	78.6	68.2	619	9.08	0.51
2	MSt <sup>c</sup>	8	62.9	16.5	31.3	1.90	0.25
3	CMS <sup>c</sup>	0.25	50.0	58.4	340	5.82	0.55
4	St/NPMI <sup>d</sup>	8	65.8	68.5	292	4.26	0.50
5	St/MA <sup>d</sup>	12	33.9	48.2	200	4.15	0.60

<sup>a</sup> Polymerization conditions:  $[\text{M}]/[\text{GMA}]/[\text{Cp}_2\text{TiCl}_2]/[\text{Zn}] = 100:1:4:8$ ,  $T = 90^\circ\text{C}$ , solvent: dioxane.

<sup>b</sup> Mark–Houwink exponent.

<sup>c</sup>  $\text{M}/\text{solvent} = 1/1$  (v/v).

<sup>d</sup> The molar ratios of St to comonomer is 1:1.  $\text{St}/\text{solvent} = 2/1$  (v/v).

too strong and irreversible coordination ability of MA with the mediator  $\text{Cp}_2\text{Ti(III)Cl}$ . The phenomenon is in consistent with the influence of ethylene carbonate solvent on St polymerization initiated from the epoxide RRO [10c]. Likewise, NPMI with a strong coordination amide group was also copolymerized with St via the initiation from the RRO reaction of GMA. A higher monomer conversion was instead obtained (entry 4), which seems to contradict the previous analysis. Thus, it is necessary to compare the molecular structures of NPMI and MA. Obviously, for NPMI comonomer, a bulky phenyl group is directly attached to nitrogen atom of the amide group. As a result, this higher steric effect can efficiently eliminate the irreversible coordination of NPMI with  $\text{Cp}_2\text{Ti(III)Cl}$ , which eventually induces a better polymerization result for St/NPMI than St/MA initiated from the GMA/ $\text{Cp}_2\text{TiCl}_2/\text{Zn}$  SCVP System. In addition, the hyperbranched polymers with higher MWs and higher PDIs were produced in all cases. Finally, lower Mark–Houwink exponents of the homopolymers and copolymers prove their hyperbranched structures. In a word, the one-pot SCVP system, GMA/ $\text{Cp}_2\text{TiCl}_2/\text{Zn}$ , can be successfully extended to other monomers for producing hyperbranched polymers.

#### 4. Conclusions

The hyperbranched polymers have been successfully prepared via a commercially available SCVP system – GMA/ $\text{Cp}_2\text{TiCl}_2/\text{Zn}$ , based on controlled/living radical polymerization mechanism (CRP). By employing an optimal  $[\text{GMA}]/[\text{Cp}_2\text{TiCl}_2]$  molar ratio to keep a low propagation chain concentration via a fast reversible termination equilibrium, the gelation did not occur until a higher level of monomers conversions. Tri-SEC and SEC as well as  $^1\text{H}$  NMR analyses confirmed that the resultant polymers possessed hyperbranched structure as evidenced by higher parameters including MWs and PDIs, and lower Mark–Houwink exponent  $\alpha$  values and lower hydrodynamic volumes compared with the linear counterparts, and hyperbranched structure were gradually formed with the progress of the polymerization. Furthermore, the polymerizations exhibited the characteristic of a CRP, i.e., the molecular weights increased with monomer conversions. The obtained hyperbranched polymers hold the epoxide-derived Ti alkoxide, vinyl, and hydroxyl end functional groups, which can be further applied to other chemical modifications and post-polymerization mechanisms. Finally, this strategy has also been efficiently extended to other monomers and provides a simple route to produce a wide range of hyperbranched polymers incorporating various physical and chemical properties.

#### Acknowledgement

The authors are grateful for subsidy provided by the National Natural Science Foundation of China (Nos. 20674080 and 20923003).

#### References

- [1] (a) Inoue K. *Prog Polym Sci* 2000;25:453–571; (b) Voit B. *J Polym Sci Part A Polym Chem* 2000;38:2505–25; (c) Jikei M, Kakimoto MA. *Prog Polym Sci* 2001;26:1233–85; (d) Gao C, Yan DY. *Prog Polym Sci* 2004;29:183–275; (e) Wang KL, Huang ST, Hsieh LG, Huang GS. *Polymer* 2008;49:4087–93; (f) Voit B. *J Polym Sci Part A Polym Chem* 2005;43:2679–99; (g) Ye JD, Ye ZB, Zhu SP. *Polymer* 2008;49:3382–92; (h) Wen YN, Jiang XS, Liu R, Yin J. *Polymer* 2009;50:3917–23.
- [2] (a) Flory PJ. *J Am Chem Soc* 1953;74:2718–23; (b) Kim YH, Webster OW. *J Am Chem Soc* 1990;112:4592–3;
- (c) Mathias LJ, Carothers TW. *J Am Chem Soc* 1991;113:4043–4; (d) Fréchet MJM, Hawker CJ, Lee R. *J Am Chem Soc* 1991;113:4583–8; (e) Percec V, Kawasumi M. *Macromolecules* 1992;25:3843–50; (f) Suzuki M, Li A, Saegusa T. *Macromolecules* 1992;25:7071–2; (g) Hult A, Malmstrom E, Johansson M. *J Polym Sci Part A Polym Chem* 1993;31:619–24.
- [3] (a) Tung LH, Hu AT, McKinley SV, Paul AM. *J Polym Sci Part A Polym Chem* 1981;19:2027–39; (b) Delassus SL, Howell BA, Cummings CJ, Dais VA, Nelson RM, Priddy DB. *Macromolecules* 1994;27:1307–12.
- [4] Fréchet MJM, Henmi M, Gitsov I, Aoshima S, Leduc MR, Grubbs RB. *Science* 1995;269:1080–3.
- [5] (a) Knauss DM, Al-Muallem HA, Huang TZ, Wu DT. *Macromolecules* 2000;33:3557–68; (b) Baskaran D. *Polymer* 2003;44:2213–20; (c) Li Y, Ryan AJ, Armes SP. *Macromolecules* 2008;41:5577–81.
- [6] (a) Simon PFW, Müller AHE. *Macromolecules* 2001;34:6206–13; (b) Simon PFW, Müller AHE. *Macromolecules* 2004;37:7548–58.
- [7] (a) Matyjaszewski K, Gaynor SG. *Macromolecules* 1997;30:7042–9; (b) Muthukrishnan S, Mori H, Müller AHE. *Macromolecules* 2005;38:3108–19; (c) Cheng KC, Chuang TH, Chang JS, Guo WJ, Su WF. *Macromolecules* 2005;38:8252–7; (d) Powell KT, Cheng C, Wooley KL. *Macromolecules* 2007;40:4509–15; (e) Mei X, Liu AH, Cui JX, Wan XH, Zhou QF. *Macromolecules* 2008;41:1264–72; (f) Ren Q, Gong FH, Jiang BB, Zhang DL, Fang JB, Guo FD. *Polymer* 2006;47:3382–9; (g) Zou P, Yang LP, Pan CY. *J Polym Sci Part A Polym Chem* 2008;46:7628–36.
- [8] (a) Wang ZM, He JP, Tao YF, Yang L, Jiang HJ, Yang YL. *Macromolecules* 2003;36:7446–52; (b) Carter S, Hunt B, Rimmer S. *Macromolecules* 2005;38:4595–603; (c) Carter S, Rimmer S, Rutkaite R, Swanson L, Fairclough JPA, Sturdy A, et al. *Biomacromolecules* 2006;7:1124–30; (d) Vogt AP, Sumerlin BS. *Macromolecules* 2008;41:7368–73; (e) Tao L, Liu JQ, Tan BH, Davis TP. *Macromolecules* 2009;42:4960–2.
- [9] (a) Hawker CJ, Fréchet MJM, Grubbs RB, Dao JL. *J Am Chem Soc* 1995;117:10763–4; (b) Tao YF, He JP, Wang ZM, Pan JY, Jiang HJ, Chen SM, et al. *Macromolecules* 2001;34:4742–8; (c) Peleshanko S, Gunawidjaja R, Petrush S, Tsukruk VV. *Macromolecules* 2006;39:4756–66.
- [10] (a) Asandei AD, Moran IW. *J Am Chem Soc* 2004;126:15932–3; (b) Asandei AD, Moran IW. *J Polym Sci Part A Polym Chem* 2006;44:1060–70; (c) Asandei AD, Moran IW, Saha G, Chen Y. *J Polym Sci Part A Polym Chem* 2006;44:2015–26.
- [11] Asandei AD, Saha G. *Macromolecules* 2006;39:8999–9009.
- [12] (a) Asandei AD, Saha G. *Polymer Prepr* 2004;45:999–1000; (b) Kong LZ, Pan CY. *Macromol Chem Phys* 2007;208:2686–97; (c) Green MLH, Lucas CR. *J Chem Soc Dalton Trans* 1972;8:1000–3; (d) Jungst R, Sekutowski D, Davis J, Luly M, Stucky J. *Inorg Chem* 1977;16:1645–55; (e) Asandei AD, Chen YH, Moran IW, Saha G. *J Organomet Chem* 2007;692:3174–82.
- [13] Rajanbabu TV, Nugent WA. *J Am Chem Soc* 1994;116:986–97.
- [14] Gansauer A, Rinker B, Barchuk A, Nieger M. *Organometallics* 2004;23:1168–71.
- [15] Friedrich J, Dolg M, Gansauer A, Geich-Gimbel D, Lauterbach T. *J Am Chem Soc* 2005;127:7071–7.
- [16] Quirk RP, Lee B. *Polym Int* 1992;27:359–67.
- [17] (a) Braunecker WA, Matyjaszewski K. *Prog Polym Sci* 2007;32:93–146; (b) Li YT, Armes SP. *Macromolecules* 2005;38:8155–62; (c) Moad G, Rizzardo E, Thang SH. *Polymer* 2008;49:1079–131.
- [18] (a) Graham S, Rannard SP, Cormack PAG, Sherrington DC. *J Mater Chem* 2007;17:545–52; (b) Dong ZM, Liu XH, Tang XL, Li YS. *Macromolecules* 2009;42:4596–603.
- [19] Podzimek S. *J Appl Polym Sci* 1994;54:91–103.
- [20] Saunders G, Cormack PAG, Graham S, Sherrington DC. *Macromolecules* 2005;38:6418–22.
- [21] (a) Besenius P, Slavin S, Vilela F, Sherrington DC. *React Funct Polym* 2008;68:1524–33; (b) Fan ZR, Lederer A, Voit B. *Polymer* 2009;50:3431–9; (c) Wang SJ, Fan XD, Kong J, Lu JR. *Polymer* 2009;50:3587–94; (d) Zhang JX, Zheng YP, Yu PY, Mo S, Wang RM. *Polymer* 2009;50:2953–7; (e) Fu Q, Cheng LL, Zhang Y, Shi WF. *Polymer* 2008;49:4981–8.
- [22] (a) Lopez-Villanueva FJ, Wurm F, Frey H. *Macromol Chem Phys* 2008;209:675–84; (b) Clarke N, De Luca E, Dodds JM, Kimani SM, Hutchings LR. *Eur Polym J* 2008;44:665–76; (c) Gong HD, Huang WY, Zhang DL, Gong FH, Liu CL, Yang Y, et al. *Polymer* 2008;49:4101–8; (d) Dong ZM, Liu XH, Lin Y, Li YS. *J Polym Sci Part A Polym Chem* 2008;46:6023–34.